This is a post-peer-review, pre-copyedit version of an article published in Iranian Polymer Journal. The final authenticated version is available online at: https://doi.org/10.1007/s13726-018-0682-x

Numerical and experimental study of Impact on a panel made of hyperelastic rubber

Amin Khodadadi¹, Gholamhossein Liaghat^{1, 2}*, Hamed Ahmadi¹, Ahmad Reza Bahramian³, Yavar Anani¹, Omid Razmkhah⁴, Samaneh Asemeni¹

¹Department of Mechanical Engineering, Tarbiat Modares University, Tehran, Iran
²School of Mechanical & Automotive Engineering, Kingston University, London, England
³Department of Polymer Engineering, Tarbiat Modares University, Tehran, Iran
⁴Coventry University, Priory Street, Coventry CV1 5FB, UK
* Corresponding author, Ghlia530@modares.ac.ir and G.Liaghat@kingston.ac.uk

Abstract

This study presents the response of rubber panels subjected to high velocity impact loading. The vulcanization characteristics of compositions have been obtained by using rheometer and the panels have been prepared at the appropriate temperature and pressure. The mechanical properties and impact performance of rubber panels is altered by the variation of compound ingredients. To investigate the effect of compound ingredients, two types of rubber panel have been prepared and mechanical properties and impact resistance of the panels have been measured by high velocity impact tests. A finite element simulation has been performed to investigate numerically the ballistic performance of rubber panels. Rubber panels was modeled by using LS-DYNA software and employing the experimental results of tensile test to characterize the behavior of rubber panel. The findings reveal a good agreement between numerical and experimental data. According to Experimental results, the ballistic limit of low and high hardness rubber panels was 80 and 94 m/s respectively that shows energy absorption of rubber panels increases as filler loading increases.

Keywords:

High velocity impact, Rubber panel, Energy absorption, Numerical simulation, Ls-Dyna, Shape of projectile.

1. Introduction

Elastomers and rubber-like materials have been used in many engineering applications over centuries. Natural rubber (NR) is flexible, an excellent puncture and tear resistance material and high damper. These features make it appropriate for impact applications [1]. Rubber panels reduce the vibrations in dynamic loading and projectile velocity in impact loading by dissipating energy via internal damping.

Rubber compounds are complex polymer systems in which several ingredients are dispersed in an elastomer matrix. Variation of compound ingredients altered the mechanical properties of rubbers [2]. One of the most important ingredients in rubber compound is the reinforcement part such as carbon black and calcium carbonate. These fillers are added to rubber formulations to improve mechanical properties [3]. Natural rubber and the reinforcing fillers, create strong interactions that lead to improvement the mechanical properties of rubber panel [4]. Li, et al. [5] carried out the quasi-static mechanical tests of three kinds of carbon black–filled tire rubbers with different matrixes by using the grid method testing system. They discussed the influences of carbon black reinforcement on the mechanical properties of rubber panels. Manroshan [6] added nano-sized calcium carbonate filler to a pre-vulcanized latex compound in different amounts and investigated the effect of filler on modulus, curing time, break elongation and tensile strength. Because of the increased interaction between the filler and rubber matrix, the curing time decreased with filler loading. Modulus at 100% and 300% elongation increased with filler loading.

In natural rubber (NR), ZnO, stearic acid, accelerators and sulfur constitute the vulcanization system. Sulfur vulcanization system was used for crosslinking of the matrix phase [7]. Nabil [8] investigated the role of various vulcanizing systems on the curing characteristics and mechanical and dynamic properties of natural rubber and ethylene–propylene–diene rubber blends. He used two accelerated sulfur-vulcanizing systems, peroxide, and mixed sulfur/peroxide-vulcanizing systems and compared them. The ZnO acts as an activator for

curing system in rubber compound [9, 10]. It increases the amount of bound sulfur and the efficiency of the crosslinking system [11].

High velocity impact-resistant materials attract the attention for the past few decades [12-14]. Impact performance is one of the major concerns in many polymer applications. Studebaker [15] studied the effects of compound ingredients on dynamic mechanical properties of rubber. He studied the major compounding variables such as the nature of rubber, the nature and amount of ingredients in curing system, the nature and amount of fillers and investigated the effect of these parameters. Sover [16] presented a new high speed falling-dart impact machine and some testing results on several elastomer like TPE, SBR, NBR/SBR and EPDM at different velocities. Fatt and Ouyang [17] conducted high velocity experiments to characterize the failure of SBR at different impact rates.

Rubbers are characterized by incompressible, hyperelastic and non-linear behavior [18]. Various models have been proposed for the simulation of rubber-like materials. The most useful formulation, is the Mooney-Rivlin model [19], where the strain energy function is expressed in terms of the invariants of the right Cauchy-Green tensor and shows an excellent agreement with experimental results.

Selvadurai [20] studied the deflection of a natural rubber membrane fixed along a circular boundary and subjected to impact loading by a rigid spherical indentor. He performed uniaxial experiments in order to characterize the constitutive behavior of the rubber material. These constitutive models were used to develop computational estimates for the quasi static loading response of a spherical indentor to determine the deflected shape of the membrane at specified load levels.

The aim of the present research work is to investigate ballistic performance and energy absorption of rubber panels. Two types of rubber panel with different compound formulation have been prepared and impact resistance of panels have been studied. Rubber panels were shot by hemispherical projectile in a velocity range of 80 to 160 m/s and residual velocity of projectile were measured. A gas gun was used to perform the tests. The finite element software LS-DYNA version 971 R4.2.1 was also used to simulate the response of rubber panels subjected to high velocity impact loading. A reasonable agreement obtained comparing the FE results to experimental findings. In order to understand the effect of projectile shape on energy absorption of panels, three types of projectile with different length to diameter ratio (L/D) and the same mass were used in numerical simulation and residual velocities of these projectiles were compared. Experimental results show that by increasing the filler loading, the ballistic performance of rubber panels improved. Also it is shown when the diameter of projectile increases, the ballistic limit and damaged area increases.

2. Experiments

2.1. Materials

Natural rubber (SMR 20) with Mooney viscosity of 65 was supplied by the Rubber Research Institute of Malaysia. Zinc oxide (ZnO), stearic acid and sulfur were obtained from LG, Korea. Fillers including carbon black (N330) and calcium carbonate was purchased from Doodeh Sanati Pars Company and Yazd Tire Company, Iran.

To understand the effect of components on mechanical properties and impact resistance of rubber panels, two types of rubber with different formulation was considered. The NR compounds formulation for 2 type of compounds are presented in Table 1.

2.2. Sample preparation

Compounding was performed on an open two-roll mixing mill (Polymix 200 L, Germany). First NR was prepared on the roller mixer at 40 rpm for about 5 minutes. Fillers include carbon black and calcium carbonate, activators include stearic acid and zinc oxide, and spindle oil added to NR gradually. Compound was homogenized at 50 rpm and 40°C for 5 minutes. Then, accelerators and a vulcanizing agent were slowly added to the mixture and mix for about 2 minutes. The vulcanization characteristics of the NR compounds were determined by a rheometer (model 4308, German zwik) at 160°C. The compounds were subsequently cured under hydraulic pressure at 160°C by a 25 tons hydraulic press (Davenport, England).

Rubber panel samples were prepared in dimension of $140 \times 140 \times 2$ mm. The areal densities of the high and low hardness samples were determined by weighing them after vulcanization. The weight of high and low hardness rubber samples are 49 and 44 g and the areal density of samples are 2.5 and 2.2 kg/m² respectively.

2.3. Tensile test

The uniaxial testing of the rubber material was carried out using tensile test machine. The ends of sample were maintained in a constrained fixed condition during extension. Uniaxial stretching test was performed on dumbbell specimens with a thickness of 2.4 mm according to ASTM D412 standard. The tensile strength tests were conducted at a crosshead speed of 500 mm/min using tensile testing machine.

The nominal stress is considered as the value of total load, measured by the load cell. Also the strain is calculated as the change in the initial gauge length. All experiments were performed at a constant uniaxial strain-rate and temperature that was approximately 22 °C.

2.4. High velocity impact tests

High-velocity impact tests were carried out using a gas gun in a velocity range of 80 to 160 m/s. All the tests were performed at room temperature and repeated three times. The gun was sighted on the target center. The exact impact velocity of each projectile was measured with a chronograph immediately before and after impacting the target. Schematic of gas-gun set up is shown in Fig. 1. All 4 sides of the specimens were constrained completely by 2 frame tighten with bolts and nuts, and then fixed in target chamber.

The projectile is hemispherical steel 4330 with diameter 10 mm and mass 9.32 g. The energy absorbed by the specimens during the penetration can be calculated from the initial and residual energy of the projectile.

Initial energy of projectile before impact (J) =
$$\frac{1}{2} m_P V_i^2$$
 (1)

Residual energy of projectile after impact (J) =
$$\frac{1}{2} m_P V_r^2$$
 (2)

Energy absorbed by target =
$$E_P(J) = \frac{1}{2} m_P (V_i^2 - V_r^2)$$
 (3)

Where E_P (J) represents the dissipated energy during the impact process, m_P (kg) is mass of projectile, V_i (m/s) is projectile initial velocity and V_r (m/s) is residual velocity.

3. Finite element analysis

The finite element software LS-DYNA version 971 R4.2.1 was used to simulate the response of rubber panel under high velocity impact. Impact velocity, projectile diameter, sample constraints and dimension were set accordingly to the experimental test. The rubber panel has dimensions of 140×140 mm and was modeled by using solid elements. The panel was clamped at four ends and subjected to impact by a hemispherical projectile of 10 mm diameter at different velocities. The projectile was modeled as a rigid body using solid elements.

3.1. Hyperelasticity

Hyperelasticity is defined as an ability of a material to experience large elastic strain due to small forces. Hyperelastic material has a nonlinear behavior and hyperelastic models are used to represent the large deformation. An elastic material is hyperelastic if there is a scalar function, denoted by $W=W(\mathbf{F})$ called strain energy function (SEF), where \mathbf{F} denotes the deformation gradient tensor. Left Cauchy–Green tensor (\mathbf{B}) and right Cauchy–Green tensor (\mathbf{C}) are expressed in $\mathbf{B}=\mathbf{FF}^{T}$ and $\mathbf{C}=\mathbf{F}^{T}\mathbf{F}$ respectively.

For Incompressible rubber Cauchy (true) stress tensor σ can be expressed as follows [3]:

$$\boldsymbol{\sigma} = -\mathbf{P}\mathbf{I} + 2\left[\left(\frac{\partial W}{\partial I_1} + I_1 \frac{\partial W}{\partial I_2}\right)\mathbf{B} - \frac{\partial W}{\partial I_2}\mathbf{B}\mathbf{B}\right]$$
(4)

Where I_1 and I_2 are the principal invariants of the left Cauchy–Green deformation tensor and P is hydrostatic pressure. For uniaxial loading conditions, the stretch is denoted by λ and the principal stretches are $\lambda_1 = \lambda$, $\lambda_2 = \lambda_3 = \lambda^{-\frac{1}{2}}$. Therefore deformation gradient tensor **F** and the left Cauchy Green deformation tensor **B** (for uniaxial loading) are:

$$\mathbf{F} = \begin{bmatrix} \lambda & 0 & 0 \\ 0 & \lambda^{-1/2} & 0 \\ 0 & 0 & \lambda^{-1/2} \end{bmatrix} \qquad \mathbf{B} = \begin{bmatrix} \lambda^2 & 0 & 0 \\ 0 & \lambda^{-1} & 0 \\ 0 & 0 & \lambda^{-1} \end{bmatrix}$$
(5)

3.2. Material modeling

LS-DYNA offers several material models for simulation of rubber-like materials. In this research Mooney-Rivlin material model is chosen, as it showed better agreement with the experimental results. Other Simulation results using these material models are given by Neves et al. [21], Pamplona et al. [22], where in all cases showing good agreement.

The Mooney–Rivlin strain energy function is given by:

$$W = C_1 (I_1 - 3) + C_2 (I_2 - 3)$$
(6)

Where are C_1 and C_2 empirically determined material constants. From Eqs. (4) and (6), the expression for stress under uniaxial loading is::

$$\boldsymbol{\sigma} = -\mathbf{P}\mathbf{I} + 2[(\mathcal{C}_1 + I_1 \ \mathcal{C}_2)\mathbf{B} - \mathcal{C}_2\mathbf{B}\mathbf{B}]$$
(7)

Where P is obtained from the condition $\sigma_{22} = 0$. The constitutive relationship is applied to one-dimensional loading by combining Eqs. (5) and (7), and this can be written as a function of the stretch λ ,

$$\sigma_{11} = (1/\lambda^2)(2 C_1 \lambda^4 + 2 C_2 \lambda^3 - 2 C_1 \lambda - 2C_2)$$
(8)

The relationship between stretch λ and engineering strain ε_{11} in the direction of the applied load is $\lambda = 1 + \varepsilon_{11}$. Tensile strength tests, were conducted on rubber specimens of two hardness (SHA45 and SHA70). The experimental data from uniaxial strength test and the least-squares technique for obtaining the best fit were used to achieve the material constants of Mooney– Rivlin constitutive model. Comparisons between empirical curves, relating true stress to engineering strain, and test data are shown in Fig. 2, which show good correlation with experimental data for both materials. Values of the parameters C_1 and C_2 for the high hardness rubber are 0.43 and 0.24 and for low hardness rubber are 0.19 and 0.02 respectively.

3.3. Mesh convergence

Before the simulations were run on the rubber panel, the mesh convergence was assessed on target. The objective is to obtain the balance between the accuracy of the mesh size and the computational time. The convergence analysis concentrated on the dimension of the elements along the thickness of panel. The parameters considered in the analysis are the residual velocity of the projectile, and the time duration of the analysis, which is directly related to the dimension of elements. Table 2 reports two different simulations, respectively with four and five elements in the thickness of panel. The residual velocities are very similar with two simulations and also the time duration of the analyses is low. Therefore, four elements in the thickness were used to insure accurate response of the panel under impact loading, while keeping the runtime low.

4. Results and discussion

4.1. Mechanical properties

Table 3 presents the mechanical properties of the high and low hardness rubber panels. By increasing the fillers loading, the mechanical properties of rubber improve. The higher values of tensile strength and lower elongation at break were observed in high hardness rubber panel.

One of the reinforcement reasons of rubber matrix by carbon black is the Van Der Waals force. Also the carbon black surface grafted the rubber chains by covalent bonds. It is caused by a reaction between the carbon black particle surface and free radicals of rubber chains. These interaction and adhesion at the rubber-filler interface also affects the reinforcement of rubber.

The hardness of the samples was measured according to ASTM D 2240 using durometer type A, and the units of hardness was expressed in shore A. Shore A hardness increased with increasing carbon-black content, as expected.

4.2. Residual velocity of Projectile

The key indicator of assessment of the kinetic energy absorbed by the target is the residual velocity of the projectile after the impact. This residual velocity is therefore the most important assessment parameter in this study.

Projectile residual velocity versus impact initial velocity for the two hardness rubbers (SHA45 and SHA70) is depicted in Fig. 3. The figure shows moderate enhancement in ballistic performance in term of lower residual velocity for the SHA70 rubber specimen compared to corresponding SHA45. This higher energy absorption capacity of high-hardness than low-hardness panels is due to the presence of a stronger molecular chains.

The ballistic limit of SHA45 and SHA70 rubber panels is 80 and 94 m/s, respectively according to experiments and 71 and 85 m/s according to numerical simulation.

4.3. Energy absorption of panels

Fig. 4 shows the energy absorption by the SHA45 and SHA70 rubber panels. As a result it can be seen that more effective performance turn out in the case of SHA70.

According to Fig. 4 with an increase in impact velocity, an increase in energy absorption was achieved. This behavior may be attributed to the fact that in high strain rates, the response of the elastomer may differ significantly from the behavior in rubbery state.

When the local segmental dynamics of the rubber become slower than the mechanical strain rate under impact loading, a transition to the glassy state and consequently brittle failure is occurred. This failure is accompanied by significant energy dissipation. Therefore, the higher velocity of the projectile is, the greater the absorption of energy by the rubber panel. This phenomenon is observed in both low and high panels.

Results show for higher velocity of projectile, difference between experimental data and numerical simulation results increases. By increasing the glass transition effect of the rubber, the error percent of numerical simulation increases. Since this effect is more evident under the high strain rate in high hardness panels, therefore, the highest error is related to the sample with high hardness under the highest impact velocity.

4.4. Specific Energy absorption

In the previous section, it was shown by increasing fillers loading, the absorbed energy in the sample increases. On the other hand, the weight of the samples is also increased. The specific energy absorption (SEA) has been evaluated to obtain the effect of the weight gain with absorbed energy. SEA is defined by the energy absorption by the sample to its areal density. Fig. 5, shows the specific energy absorption of samples that is calculated from equation 9.

Specific energy absorption =
$$\frac{\frac{1}{2} m V_b^2}{\text{Areal density}}$$
 (9)

Where V_b is ballistic limit velocity and it is defined as the minimum velocity required to penetrate a target. The specific energy absorption of low and high hardness rubber panel was evaluated.

As it can be seen, SEA of high hardness rubber is higher than low hardness one. Although high hardness specimens have the higher weight than low hardness rubber samples, the amount of energy absorbed is higher than others, and therefore the SEA is higher. Therefore, the use of a high hardness rubber panel as an impact resistance is reasonable.

4.5. Rubber panel deformation

Fig. 6 shows the deformation and perforation of the rubber panels. After the projectile strikes the target, rubber deforms and reduces the projectile velocity. If an elastomer deformed at sufficiently high strain rates, it enters the glass transition zone of the viscoelastic range [23]. Deformation is highly localized causing plug formation. By increasing the projectile's velocity, the transition of rubber panel to glassy state is more significant. As a result the plug formation of the sample increases. In Table 4, the mass of the separated plugs from high and low hardness samples under impact velocity of 151 m/s is presented.

The glass transition in rubber is affected by the incorporation of reinforcing fillers such as carbon black. As it is shown for low hardness samples the separated mass doesn't vary by projectile velocity. Glassy state is not significant due to low filler loading.

5. Effect of projectile shape on impact resistance of rubber panels

Shape of the projectile is a major factor influencing the energy absorption and impact resistance offered by the rubber panel. To compare the impact resistance of rubber panels against hemispherical projectiles with different length to diameter (L/D) ratio, numerical simulations were performed. In order to keep a constant mass, the length of the projectile changed depending on the projectile diameter. In this study, three projectiles, Fig. 7, have been used to analyze the influence of projectile diameter on the penetration performance of rubber panels. For each projectile, the mass is kept as constant $m_p=9.32$ g.

Initial and residual velocity curves of various shape of the projectiles are plotted to evaluate the energy absorption capacity of the rubber panels. Figs. 8 shows the comparison of projectiles with diameter of 8, 10 and 12 mm as a result of impact on SHA70 and SHA45 rubber panels. It is shown that with increasing the diameter of projectile the residual velocity decreases. So the projectile with diameter of 12 mm is the most efficient penetrator of the rubber panel and consequently the lowest residual velocity is achieved with an equal initial velocity while projectile with 8 mm diameter is related to the highest residual velocity. These results valid for both of SHA45 and SHA70 rubber panels.

At low impact velocities, the difference between the impact and residual velocities is greater in case of the projectile with diameter of 12 mm. But as the impact velocity is increased, the velocity drop curves (difference between the impact and residual velocities) of projectiles overlap and in high velocities it can be expected that the residual velocities will be the same for projectiles with different shapes.

Based on the results of each series of test, the ballistic limit, V_{bl} , was determined as the average between the highest impact velocity that projectile don't perforate and the lowest impact velocity that projectile perforate the rubber panel. The ballistic limit of SHA45 rubber panel for projectile with diameter of 8, 10 and 12 mm was 63, 70 and 78 m/s and for SHA70 rubber panel was 77, 85 and 89 m/s respectively. The results clearly show that the ballistic limit velocity increases for rubber panel with higher hardness. Also using projectiles with larger diameter lead to higher ballistic limit.

It is found that the residual velocity of projectile with diameter of 12mm decreased more as compared to other projectiles (projectile with diameter of 8 and 10mm) for every incidence velocity. Therefore, energy absorption in the target plate increases as the projectile shape changes from small to large diameter; or in other word, energy absorption increases with increasing contact surface area of the projectile at impact point on the target. The energy absorption of the panel is describe as the loss of kinetic energy of the projectile. In Fig. 9, energy absorption of SHA45 and SHA70 rubber panels at ballistic limit velocity is shown.

Fig. 10 displays the variation of three projectile velocity with time at impact velocity of 120 m/s for the SHA70 and SHA45 rubber panels. All projectiles penetrate through the rubber panels with their residual velocities decreasing in the following order: projectile with diameter of 12 mm, 10 mm and 8 mm.

A few observations are notable from Fig. 10 as follows:

(i) The rate of deceleration of the projectile with larger diameter is always higher than that of the smaller projectile,

(ii) The projectile with larger diameter has a lower residual velocity on impact with the same target,

(iii) The projectile with smaller diameter penetrate the rubber panel in less time,

(iv) Time duration of penetration is longer for SHA45 rubber panel,

(v) For low hardness rubber, the gradient was gentle due to low module and large elongation to failure.

The panel deformation of high hardness rubber panel are compared for various projectiles to study the effect of projectile's shape on the rubber deformation (Figs. 11(a)–(c)). The elements located at the middle zone of the rubber panel fail when stress/strain level exceeds the failure strength set by the constitutive model and are eliminated from the simulation. The bullet during penetration causes large strain in the target which is responsible for the plug formation. It is observed that the damage zone in the rubber panel increases as the projectile diameter increases. It is due to increase in the contact surface area of projectile to the rubber panel. It is also found that the energy absorption in the target increases with increase in the contact surface area of the projectile. This absorbed energy in the rubber panel appears in form of damages.

6. Conclusion

In present study, the ballistic performance of rubber panels has been investigated. Two types of rubber panel with different compound ingredients were prepared and high-velocity impact test was conducted on rubber panels. Residual velocity of projectile was obtained and ballistic limit and energy absorption of panels have been investigated by experimental and numerical methods. A numerical simulation also have been performed to compare the impact resistance of rubber panels against hemispherical projectiles with different length to diameter (L/D) ratio. The following conclusions can be made from the study:

- 1- More effective performance turn out in high hardness rubber panel in which the ballistic limit is 17.5% higher than low hardness panel. Reinforcing rubber by fillers like carbon black improve energy absorption capability significantly.
- 2- The plug formed under impact loading increases by increase of projectile's velocity especially for high hardness rubber panel.
- 3- Energy absorption of target plate increases as the projectile's shape changes from small to large diameter. This absorbed energy in the rubber panel appears in form of damages. It can be concluded that the damage zone in the rubber panel increases as the projectile diameter increases.

Acknowledgements

The authors are grateful to the Tarbiat Modares University (TMU) for their financial support.

References

- [1] Vergnaud J-M, Rosca I-D (2016) Rubber curing and properties: CRC Press.
- [2] Bhattacharya M, Bhowmick AK (2010) Synergy in carbon black-filled natural rubber nanocomposites. Part I: Mechanical, dynamic mechanical properties, and morphology. materials science 45:6126-38.

- [3] Fröhlich J, Niedermeier W, Luginsland H-D (2005) The effect of filler–filler and filler–elastomer interaction on rubber reinforcement. Composites Part A: Applied Science and Manufacturing 36:449-60.
- [4] Leblanc JL (2002) Rubber–filler interactions and rheological properties in filled compounds. Progress in polymer science 27:627-87.
- [5] Li X, Li Z, Xia Y (2015) Test and calculation of the carbon black reinforcement effect on the hyper-elastic properties of tire rubbers. Rubber Chemistry and Technology 88:98-116.
- [6] Manroshan S, Baharin A (2005) Effect of nanosized calcium carbonate on the mechanical properties of latex films. Journal of Applied Polymer Science 96:1550-6.
- [7] Visakh P, Thomas S, Oksman K, Mathew AP (2012) Crosslinked natural rubber nanocomposites reinforced with cellulose whiskers isolated from bamboo waste: Processing and mechanical/thermal properties. Composites Part A: Applied Science and Manufacturing 43:735-41.
- [8] Nabil H, Ismail H, Azura A (2014) Properties of natural rubber/recycled ethylene–propylene– diene rubber blends prepared using various vulcanizing systems. Iranian Polymer Journal 23:37-45.
- [9] Brydson JA (1978) Rubber chemistry: Applied Science Publishers.
- [10] Li Z, Zhang J, Chen S (2008) Effects of carbon blacks with various structures on vulcanization and reinforcement of filled ethylene-propylene-diene rubber. Express Polym Lett 2:695-704.
- [11] Luyt AS, McGill WJ, Shillington D (1990) DSC study of the interaction of 2mercaptobenzothiazole, sulphur, ZnO and stearic acid in the absence of rubber. Polymer International. 23:135-9.
- [12] Khodadadi A, Liaghat GH, Sabet AR, Hadavinia H, Aboutorabi A, Razmkhah O (2018) Experimental and numerical analysis of penetration into Kevlar fabric impregnated with shear thickening fluid. J Thermoplastic Composite Materials 31:392-407.
- [13] Moallemzadeh AR, Sabet AR, Abedini H (2017) Mechanical and morphological study of polymer composite plates having different fiber surface treatments with particular response to high velocity projectile impact. Iranian Polymer Journal 26:229-38.
- [14] Mamivand M, Liaghat G (2010) A model for ballistic impact on multi-layer fabric targets. International Journal of Impact Engineering 37:806-12.
- [15] Studebaker M, Beatty J (1974) Effects of compounding on dynamic mechanical properties of rubber. Rubber Chemistry and Technology 47:803-24.
- [16] Söver A, Frormann L, Kipscholl R (2009) High impact-testing machine for elastomers investigation under impact loads. Polymer Testing 28:871-4.
- [17] Fatt MSH, Ouyang X (2007) Integral-based constitutive equation for rubber at high strain rates. Solids and structures 44:6491-506.
- [18] Sasso M, Palmieri G, Chiappini G, Amodio D (2008) Characterization of hyperelastic rubberlike materials by biaxial and uniaxial stretching tests based on optical methods. Polymer Testing 27:995-1004.
- [19] Mooney M (1940) A theory of large elastic deformation. J applied physics 11:582-92.
- [20] Selvadurai A (2006) Deflections of a rubber membrane. Mechanics and Physics of Solids 54:1093-119.

- [21] Neves R, Micheli G, Alves M (2010) An experimental and numerical investigation on tyre impact. impact engineering 37:685-93.
- [22] Pamplona D, Goncalves P, Lopes S (2006) Finite deformations of cylindrical membrane under internal pressure. Mechanical Sciences 48:683-96.
- [23] Roland CM (2012) Glass Transition in Rubbery Materials. Rubber Chemistry and Technology 85:313-26.

Fig. 1 Schematic set-up of gas-gun.

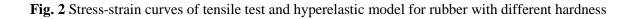


Fig. 3 Residual velocities versus initial velocity for SHA45 and SHA70 rubber panel

Fig. 4 Energy absorption performance for high and low hardness rubber panel

Fig. 5 Specific energy absorption performance for high and low hardness rubber panel

Fig. 6 Images of damaged specimens under projectile velocity of 151 m/s (a) SHA45 rubber panel (b) SHA70 rubber panel

Fig. 7 Shapes and dimensions of the various projectiles used in numerical simulations

Fig. 8 Residual velocity versus initial velocity for impact of projectiles with different diameters on SHA45 and SHA70 rubber panel

Fig. 9 Energy absorption of SHA45 and SHA70 rubber panels at ballistic limit velocity

Fig. 10 Comparison of projectile velocity histories at impact velocity of 120 m/s

Fig. 11 Predicted deformation characteristics of high hardness rubber panel (a) projectile with diameter of 8mm (b) projectile with diameter of 10mm (c) projectile with diameter of 12mm

	_			
Ingredients	Loading (Phr)			
Ingreatents	Formulation 1	Formulation 2		
NR	100	100		

Table 1 Formulation of compounds

Carbon Black (N330)	60	40
Zink oxide	5	5
Calcium carbonate	30	30
Spindle oil	15	30
Sulfur	2	1.5
Volcacit	0.7	0.7

Table 2 Rubber panel simulation results with four and five elements in thickness

Element in Thickness	Initial velocity (m/s)	Residual velocity (m/s)	Analysis duration	Number of elements	Element dimension (mm)
5	160	141.1	0.00056	200000	0.5×0.5×0.4
4	160	141.5	0.00056	160000	0.5×0.5×0.5

Table 3 Mechanical properties of rubber

Material	Tensile Strength (MPa)	Elongation (%)	Hardness (Shore A)	Stress (100 %) (MPa)	Stress (200 %) (MPa)	Stress (300 %) (MPa)
High hardness rubber	9.08	218.10	70	3.59	8.33	0
Low hardness rubber	8.38	347.80	45	1.41	3.44	6.57

Table 4 Plug	separated	from target	under pr	rojectile	impact

	Specimen number	V _i (m/s)	Plug mass (g)
HH Rubber Panel	1	151	0.21

	2	127	0.17
	3	115	0.06
	4	85	0
	1	151	0.03
LH Rubber Panel	2	127	0.03
LH Rubbel Fallel	3	110	0.02
	4	70	0